Series-coupled silicon racetrack resonators and the Vernier effect: theory and measurement

Robi Boeck,[1,*] **Nicolas A. F. Jaeger,**[1] **Nicolas Rouger,**[1,2] **and Lukas Chrostowski**[1]

[1]*Department of Electrical and Computer Engineering, University of British Columbia, Vancouver, British Columbia, Canada*

[2]*Currently at Centre National de la Recherche Scientifique, Grenoble Electrical Engineering Lab, Grenoble University, France*

**rboeck@ieee.org*

Abstract: Silicon-on-insulator racetrack resonators can be used as multiplexers in wavelength division multiplexing applications. The free spectral range should be comparable to the span of the C-band so that a maximum number of channels can be multiplexed. However, the free spectral range is inversely proportional to the length of the resonator and, therefore, bending losses can become non-negligible. A viable alternative to increase the free spectral range is to use the Vernier effect. In this work, we present the theory of series-coupled racetrack resonators exhibiting the Vernier effect. We demonstrate the experimental performance of the device using silicon-on-insulator strip waveguides. The extended free spectral range is 36 nm and the interstitial peak suppression is from 9 dB to 17 dB.

OCIS codes: (130.0130) Integrated optics; (130.7408) Wavelength filtering devices; (230.5750) Resonators.

References and links

1. L. Zhang, Y. Li, M. Song, J. Yang, R. Beausoleil, and A. Willner, "Silicon microring-based signal modulation for chip-scale optical interconnection," Appl. Phys. A **95**, 1089–1100 (2009).
2. F. Xia, M. Rooks, L. Sekaric, and Y. Vlasov, "Ultra-compact high order ring resonator filters using submicron silicon photonic wires for on-chip optical interconnects," Opt. Express **15**, 11934–11941 (2007).
3. P. Dong, W. Qian, H. Liang, R. Shafiiha, N. Feng, D. Feng, X. Zheng, A. V. Krishnamoorthy, and M. Asghari, "Low power and compact reconfigurable multiplexing devices based on silicon microring resonators," Opt. Express **18**, 9852–9858 (2010).
4. M. S. Dahlem, C. W. Holzwarth, A. Khilo, F. X. Kartner, H. I. Smith, and E. P. Ippen, "Eleven-channel second-order silicon microring-resonator filterbank with tunable channel spacing," in Conference on Lasers and Electro-Optics, OSA Technical Digest (CD) (Optical Society of America, 2010), paper CMS5.
5. M. Popovic, T. Barwicz, M. Dahlem, F. Gan, C. Holzwarth, P. Rakich, H. Smith, E. Ippen, and F. Kartner, "Tunable, fourth-order silicon microring-resonator add-drop filters," IET Digest **123**, (2007).
6. B. Timotijevic, G. Mashanovich, A. Michaeli, O. Cohen, V. M. N. Passaro, J. Crnjanski, and G. T. Reed, "Tailoring the spectral response of add/drop single and multiple resonators in silicon-on-insulator," Chin. Opt. Lett. **7**, 291–295 (2009).
7. L. Jin, M. Li, and J. He, "Experimental investigation of waveguide sensor based on cascaded-microring resonators with Vernier effect," in 2010 Conference on Lasers and Electro-Optics (CLEO) and Quantum Electronics and Laser Science Conference (QELS), 1–2 (2010).
8. P. Koonath, T. Indukuri, and B. Jalali, "3-D integrated Vernier filters in silicon," in Integrated Photonics Research and Applications/Nanophotonics, Technical Digest (CD) (Optical Society of America, 2006), paper IMG1.

9. T. Chu, N. Fujioka, S. Nakamura, M. Tokushima, and M. Ishizaka, "Compact, low power consumption wavelength tunable laser with silicon photonic-wire waveguide micro-ring resonators," in 35th European Conference On Optical Communication (ECOC), 1–2 (2009).
10. R. Boeck, N. A. F. Jaeger, and L. Chrostowski, "Experimental Demonstration of the Vernier Effect using Series-Coupled Racetrack Resonators," in 2010 International Conference on Optical MEMS & Nanophotonics (2010).
11. D. G. Rabus, *Integrated Ring Resonators: The Compendium*, 1st ed. (Springer, 2007).
12. N. Rouger, L. Chrostowski, and R. Vafaei, "Temperature Effects on Silicon-on-Insulator (SOI) Racetrack Resonators: A Coupled Analytic and 2-D Finite Difference Approach," J. Lightwave Technol. **28**, 1380–1391 (2010).
13. H. H. Li, "Refractive index of silicon and germanium and its wavelength and temperature derivatives," J. Phys. Chem. Ref. Data **9**, 561 (1980).
14. C. Z. Tan and J. Arndt, "Temperature dependence of refractive index of glassy SiO2 in the infrared wavelength range," J. Phys. Chem. Solids **61**, 1315–1320 (2000).
15. O. Schwelb, "The nature of spurious mode suppression in extended FSR microring multiplexers," Opt. Commun. **271**, 424–429 (2007).
16. C. Chaichuay, P. P. Yupapin, and P. Saeung, "The serially coupled multiple ring resonator filters and Vernier effect," Opt. Appl. **XXXIX**, (2009).
17. W. Bogaerts, R. Baets, P. Dumon, V. Wiaux, S. Beckx, D. Taillaert, B. Luyssaert, J. V. Campenhout, P. Bienstman, and D. V. Thourhout, "Nanophotonic Waveguides in Silicon-on-Insulator Fabricated With CMOS Technology," J. Lightwave Technol. **23**, 401 (2005).
18. P. Dumon, W. Bogaerts, V. Wiaux, J. Wouters, S. Beckx, J. Van Campenhout, D. Taillaert, B. Luyssaert, P. Bienstman, D. Van Thourhout, and R. Baets, "Low-Loss SOI Photonic Wires and Ring Resonators Fabricated With Deep UV Lithography," IEEE Photon. Technol. Lett. **16**, 1328–1330 (2004).
19. M. A. Popovic, E. P. Ippen, and F. X. Kartner, "Universally balanced photonic interferometers," Opt. Lett. **31**, 2713–2715 (2006).
20. A. Fallahkhair, K. S. Li, and T. E. Murphy, "Vector Finite Difference Modesolver for Anisotropic Dielectric Waveguides," J. Lightwave Technol. **26**, 1423–1431 (2008).
21. P. Dumon, "Ultra-Compact Integrated Optical Filters in Silicon-on-insulator by Means of Wafer-Scale Technology," PhD Thesis, Universiteit Gent, (2007).

1. Introduction

The increasing demand for data bandwidth has resulted in the need for cost-effective interconnects inside the electronic chips of high performance computing systems. The typical metallic interconnects currently used in high speed electronic chips are expected to pose a bottleneck to future development; as the clock rate increases, high power consumption and long latency occurs [1]. A possible solution is to use optical interconnection devices. Ideally, one would want to monolithically integrate optics and electronics on a single, silicon platform. This would combine the advantages of high density electronics and high speed photonics giving significant performance enhancements, cost reductions and a possible solution to the abovementioned bottleneck. Silicon-on-insulator (SOI) interconnection devices provide a viable method to achieve these design goals. To reduce the amount of silicon real estate needed for optical signal routing, wavelength division multiplexing (WDM) based on SOI microring resonators is a possible solution [2–5]. The high-index-contrast of SOI enables sub-micrometer waveguide dimensions as well as the radii of microring resonators to be as small as a few micrometers while ensuring low loss and single mode propagation. Recently, a 1st order, thermally tunable, two channel multiplexer based on SOI racetrack resonators was fabricated [3]. This multiplexer has a free spectral range (FSR) of 19 nm and an out-of-band rejection ratio of approximately 22 dB [3]. However, a box-like drop port response is desired. One method to both increase the out-of-band rejection ratio and improve the flatness of the drop port response, is to use series-coupled microring resonators [2,4,5]. Recently, 2nd order [4], 4th order [5], and 5th order [2] multiplexers have been fabricated showing a marked improvement in the flatness of the drop port response as well as out-of-band rejection ratios of 32 dB to 40 dB. However, these multiplexers have relatively small FSRs ranging from 16 nm to 18 nm. Ideally, an FSR comparable to the span of the C-band would be beneficial, as this would increase the number of channels that could be multiplexed or demultiplexed; two series-coupled microring resonators that have different

total lengths can be used to achieve this due to the Vernier effect. Series-coupled microring resonators showing the Vernier effect have been fabricated [6–10]. To the best of our knowledge, only five research groups have shown the Vernier effect using the SOI platform [6–10]. B. Timotijevic et al. [6], L. Jin et al. [7] and P. Koonath et al. [8] showed weak interstitial peak suppression. T. Chu et al. fabricated a silicon wavelength tunable laser using an external double microring resonator [9]. We have demonstrated series-coupled SOI strip waveguide racetrack resonators with an extended FSR of 36.2 nm and an improvement in the interstitial peak suppression of greater than 11 dB [10].

In this paper, we present an explanation of the theory and experimental results of the Vernier effect using series-coupled racetrack resonators using SOI strip waveguides. We have gathered both theoretical aspects and experimental results within the same paper, coupled to an improvement in a Vernier effect device. For the purpose of comparison, we present measurements made on individual racetrack resonators having the same dimensions as the resonators within the Vernier effect device in order to show that the Vernier effect, in fact, has been achieved.

2. Theory

The FSR of a racetrack resonator is inversely proportional to the length of the resonator. If the FSR of a single resonator is comparable to the span of the C-band, the bending losses can become quite large and, thus, reduce the performance of the device. However, the Vernier effect can be used to extend the FSR. The Vernier effect can be created by using series-coupled racetrack resonators. The device consists of two bus waveguides connected to two series-coupled racetrack resonators with different lengths. Ideally, one would like these devices to have low-losses, small foot-prints, extended FSRs that are comparable to the C-band, and to exhibit large interstitial peak suppressions.

The drop port transfer function that is used to model the Vernier effect device can be determined by [11]

$$TF_{drop} = \frac{i(\kappa_1\kappa_2\kappa_3 X_1 X_2)^{1/2}}{1 - t_1 t_2 X_1 - t_2 t_3 X_2 + t_1 t_3 X_1 X_2}, \tag{1}$$

where $X_i = exp(-\alpha L_i/2 + i\varphi_i)$, $t_i = (1-\kappa_i)^{1/2}$, $\varphi_i = (2\pi n_g L_i)/\lambda$, α [/m] is the total loss coefficient, L_1 [m] and L_2 [m] are the total lengths of the first and second racetrack resonator, respectively, λ is the wavelength, n_g is the group index, κ_1 and κ_3 are the symmetric (real) point power coupling factors to the bus waveguides, and κ_2 is the (real) point inter-ring power coupling factor. n_g is given by [11]

$$n_g(\lambda, \mathrm{T}) = n_{eff}(\lambda, \mathrm{T}) - \lambda \frac{\delta n_{eff}(\lambda, \mathrm{T})}{\delta \lambda}, \tag{2}$$

where n_{eff} is the effective index and T is temperature. n_{eff} is λ and T dependent since the refractive indices of Si and SiO_2 are functions of λ and T. n_{eff} can be calculated using a mode solver and the λ and T dependency of the refractive indices can be modeled using experimental data [12–14].

The extended FSR needs to be comparable to the span of the C-band (35 nm) to maximize the number of channels that can be multiplexed. The extended FSR is related to the FSR of each racetrack resonator by [15, 16]

$$FSR_{extended} = m_1 FSR_1 = m_2 FSR_2, \tag{3}$$

where m_1 and m_2 are co-prime integers. The total length of each racetrack resonator is determined by using

$$\frac{m_2}{m_1} = \frac{L_2}{L_1}. \tag{4}$$

One must optimize the performance of the device by ensuring: (1) the removal of twin resonance peaks located between the main resonance peaks; (2) that the main resonance peak intensity is high (i.e. ensuring low insertion loss); (3) that there is minimal splitting of the main resonance peak; and (4) that there is large interstitial peak suppression as shown in Fig. 1(a) and Fig. 1(b). The twin peaks shown in Fig. 1(a) occur because m_1 and m_2 are chosen to be 9 and 7, respectively. To remove the occurrence of the twin peaks, m_2 should be equal to m_1-1 (assuming $m_1 > m_2$). The optimized device shown in Fig. 2(a) has an interstitial peak suppression greater than 41.8 dB which is sufficient for WDM applications. Figure 2(b) shows that the optimized device does not have any main resonance peak splitting. If we increase m_1 (and m_2), the interstitial peak suppression decreases. Thus, m_1 needs to be small enough to give adequate interstitial peak suppression. The choice of L_1 and L_2 determines the extended FSR. The power coupling factors need to be optimized to obtain high main resonance intensity, minimal main resonance splitting, and large interstitial peak suppression [15,16].

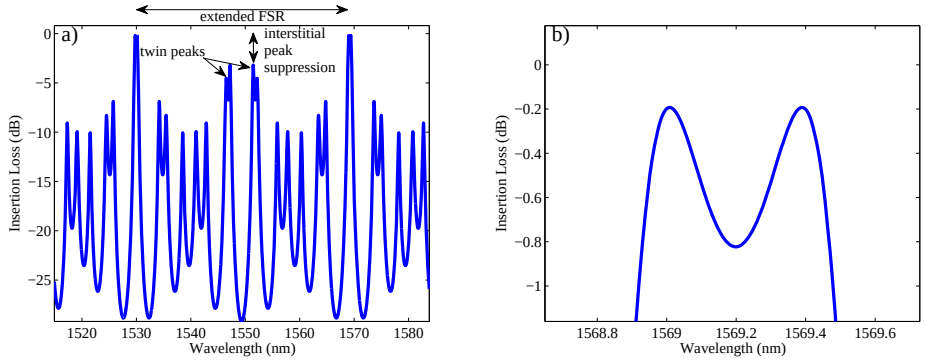

Fig. 1. (a) Theoretical drop port response of the un-optimized device illustrating the twin peaks, extended FSR, and minimum interstitial peak suppression, and (b) the main resonance peak splitting. The design parameters are m_1 and m_2 are 9 and 7, respectively. L_1 and L_2 are 127.91 μm and 99.487 μm, respectively. κ_1, κ_2 and κ_3 are 0.35, 0.1, and 0.35, respectively. The waveguide width is 500 nm, the propagation loss is 3 dB/cm, and n_g is 4.306.

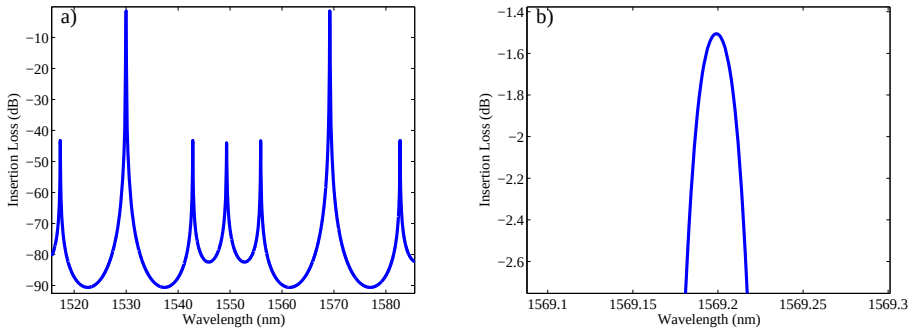

Fig. 2. (a) Theoretical drop port response of the optimized device illustrating large interstitial peak suppression and (b) no main resonance splitting. The design parameters are m_1 and m_2 are 3 and 2, respectively. L_1 and L_2 are 42.637 μm and 28.425 μm, respectively. κ_1, κ_2 and κ_3 are 0.015, 0.00005, and 0.015, respectively. The waveguide width is 500 nm, the propagation loss is 3 dB/cm, and n_g is 4.306.

3. Experimental results

Our device was fabricated using 193 nm lithography. To couple light into and out of the waveguides, 1-D periodic grating couplers with 400 μm long tapers (to ensure single mode propagation for the TE-polarization) are used [17]. The SOI strip waveguides have a width of 420 nm, a height of 220 nm, and a buried oxide (BOX) thickness of 2 μm. These waveguide dimensions typically result in about 20 dB/cm propagation loss [18]. Although the losses are large compared to a 500 nm width waveguide, the benefit to having a 420 nm waveguide is that the mode is less confined so the gap distances can be increased to reduce the chances of fabrication errors while keeping the power coupling factors relatively the same. We choose to set m_2 = 4 and m_1 = 5 (ratio equal to 0.8), which turns out to be the same values as given in [16]. The straight sections of the racetrack resonator, L_c, are 15 μm. The radii (defined from the centers of the waveguides), R_1 and R_2, of the half-circle sections of the racetrack resonators are 6.545 μm and 4.225 μm, respectively. A small straight section of 50 nm is added to the middle of each half-circle of the racetrack resonator. This straight section was inserted so that several devices with different total resonator lengths (different straight section length) could be fabricated while the power coupling factors remained the same. However, this straight section can increase the scattering losses. The ratio of L_2 to L_1 is 0.7953. The gap distances for the inter-ring coupling region and the two coupling regions to the bus waveguides are approximately 410 nm and 230 nm, respectively. Figure 3 shows scanning-electron micrographs (SEMs) of the fabricated device.

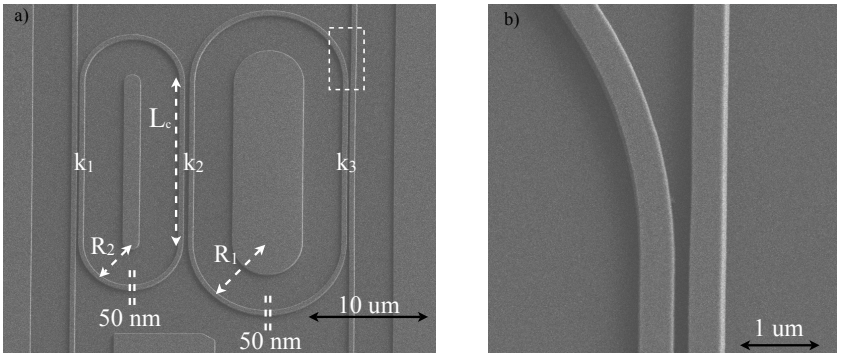

Fig. 3. SEM of (a) fabricated series-coupled racetrack resonators, and (b) coupling region.

Figure 4(a) shows the measured drop port response of the series-coupled racetrack resonator. Figure 4(c) shows the straight waveguide transmission response that was used for calibration. The extended FSR is 35.96 nm, the quality factor is 2084, the 3-dB bandwidth is 0.74 nm, there is minimal splitting of the main resonance peak [shown in Fig. 4(b)], and the interstitial peak suppression is between 9.11 dB and 17.11 dB. Thus, we can conclude that using series-coupled racetrack resonators provide a marked improvement in the FSR compared to single racetrack resonator multiplexers. The measured through port response showed an extinction ratio of 5.43 dB. Although the interstitial peak suppression of our device shows a marked improvement compared to other devices reported in literature, the suppression is still insufficient for many WDM applications. In order to improve suppression in future devices, we intend to increase the gap distances with the inter-ring gap distance having the greatest impact on the suppression. Also, the Vernier effect exhibited in devices such as the one reported here may effect the through port channels due to the increase in dispersion and group delay [19]. A new Vernier scheme proposed by M. Popovic et al. may provide a potential solution to this problem [19].

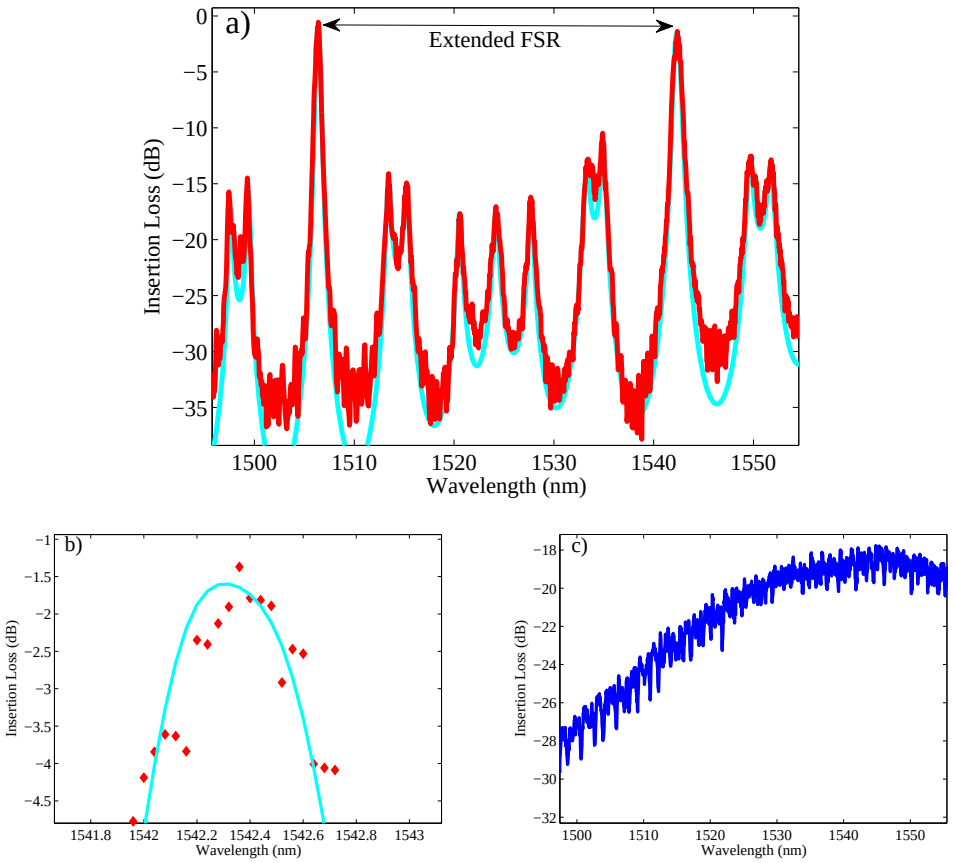

Fig. 4. (a) Experimental (red) and curve-fit (cyan) drop port response for series-coupled racetrack resonators, (b) shows the minimal main resonance splitting (zoom in of Fig. 3a), and (c) shows the straight waveguide transmission response used for calibration.

The following presents the details for curve-fitting the results shown in Fig. 4(a). The device shown in Fig. 3 has a waveguide width of approximately 420 nm and gap distances of approximately 410 nm and 230 nm and, hence, these are the values used here. Using a 2D Finite Difference (FD) mode solver [20], the group index is 4.5473. The best fit between the model and the experiment is for κ_1 = 0.3665, κ_2 = 0.02485 and κ_3 = 0.3665. From these values, we determine the gap distances using supermode analysis to be between 405 nm and 410 nm for the inter-ring coupling region and between 230 nm and 235 nm for the two coupling regions to the bus waveguides, which are very close to the values determined from the SEM images in Fig. 3(a) and Fig. 3(b). The curve-fit takes into account the wavelength dependency of the power coupling factors using the 2D FD mode solver.

The slight mismatch between the curve-fit and the experimental results may be due to various assumptions and unknown experimental waveguide characteristics. These assumptions and characteristics include: (1) The waveguides are assumed to be perfectly rectangular (however, cross-sectional SEM images of similar SOI waveguides have shown that the sidewalls can have slopes of approximately 9^o [21] and a trapezoidal waveguide structure will change the effective index as well as the gap distances); (2) the group index is assumed to be wavelength independent; (3) the height of the waveguide is assumed to be 220 nm; (4) the waveguide curvature is

neglected for n_{eff} calculations; and (5) the distance between waveguides is not considered for n_{eff} calculations.

To evaluate and confirm the existence of the Vernier effect, individual racetrack resonators with the same structural designs as those that constitute the Vernier-effect device were fabricated on the same die. Figure 5 shows the experimental drop port response of the two racetrack resonators which was calibrated using a straight waveguide transmission response. The quality factors for the racetrack resonators with a radius of 6.545 μm and 4.225 μm are approximately 1091 and 1157, respectively. The periodic resonance peaks of both racetrack resonators overlap at 1502.44 nm and 1538.24 nm. The difference between these two resonance wavelengths is 35.8 nm, which is close to value of the extended FSR shown in Fig. 4(a).

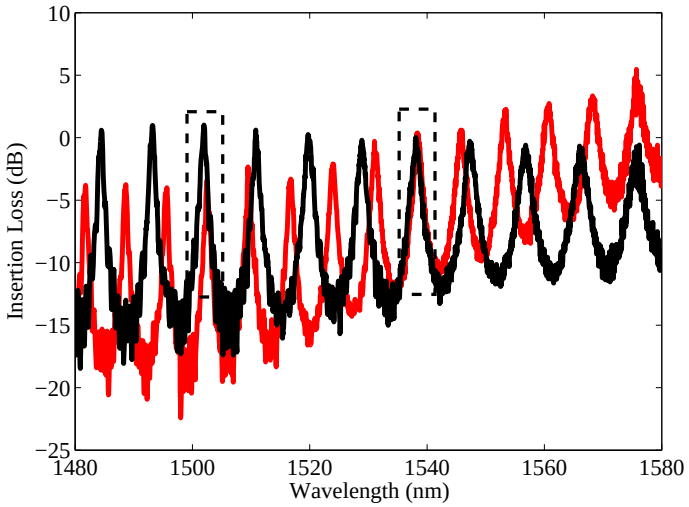

Fig. 5. Experimental drop port response for single racetrack resonators with a radius of 6.545 μm (red) and 4.225 μm (black).

4. Summary

In summary, we have presented the theory of series-coupled racetrack resonator showing the Vernier effect. Our experimental results for the series-coupled racetrack resonator showed an extended FSR of 36 nm, no twin resonance peaks, minimal splitting of the main resonance peaks, interstitial peak suppression from 9 dB to 17 dB, a quality factor of 2084, and a 3-dB bandwidth of 0.74 nm. Individual racetrack resonators similar to those that constitute the Vernier-effect device were fabricated. The resonance peaks overlap at 1502.44 nm and 1538.24 nm with a difference close to the extended FSR of the series-coupled racetrack resonators.

Acknowledgements

We would like to thank the Natural Sciences and Engineering Research Council of Canada (CGS-M) for partial support of this project. The authors would also like to thank Raha Vafaei and Stephanie Flynn for obtaining SEM images, Miguel Ángel Guillén Torres for the many insightful discussions, and Nadia Makan for helping to build the experimental set-up. We would also like to acknowledge CMC Microsystems and Lumerical Solutions Inc. for supporting this project, as well as ePIXfab at IMEC for the fabrication of our devices.